
Coded Residual Transform for Generalizable Deep Metric Learning

Shichao Kan¹, Yixiong Liang¹, Min Li¹, Yigang Cen^{2,3,*}, Jianxin Wang¹, Zhihai He^{4,5,*}

¹School of Computer Science and Engineering, Central South University, Changsha, Hunan, 410083

²Institute of Information Science, School of Computer and Information Technology,
Beijing Jiaotong University, Beijing 100044, China

³Beijing Key Laboratory of Advanced Information Science and Network Technology, Beijing 100044, China

⁴Department of Electrical and Electronic Engineering, Southern University of Science and Technology,
Shenzhen, China

⁵Pengcheng Lab, Shenzhen, 518066, China

kanshichao@csu.edu.cn, yxliang@csu.edu.cn, limin@mail.csu.edu.cn
ygcen@bjtu.edu.cn, jxwang@mail.csu.edu.cn, hezh@sustech.edu.cn

Abstract

A fundamental challenge in deep metric learning is the generalization capability of the feature embedding network model since the embedding network learned on training classes need to be evaluated on new test classes. To address this challenge, in this paper, we introduce a new method called *coded residual transform* (CRT) for deep metric learning to significantly improve its generalization capability. Specifically, we learn a set of diversified prototype features, project the feature map onto each prototype, and then encode its features using their projection residuals weighted by their correlation coefficients with each prototype. The proposed CRT method has the following two unique characteristics. First, it represents and encodes the feature map from a set of complimentary perspectives based on projections onto diversified prototypes. Second, unlike existing transformer-based feature representation approaches which encode the original values of features based on global correlation analysis, the proposed coded residual transform encodes the relative differences between the original features and their projected prototypes. Embedding space density and spectral decay analysis show that this multi-perspective projection onto diversified prototypes and coded residual representation are able to achieve significantly improved generalization capability in metric learning. Finally, to further enhance the generalization performance, we propose to enforce the consistency on their feature similarity matrices between coded residual transforms with different sizes of projection prototypes and embedding dimensions. Our extensive experimental results and ablation studies demonstrate that the proposed CRT method outperform the state-of-the-art deep metric learning methods by large margins and improving upon the current best method by up to 4.28% on the CUB dataset.

1 Introduction

Deep metric learning (DML) aims to learn effective features to characterize or represent images, which has important applications in image retrieval [1, 2], image recognition [3], person re-identification [4], image segmentation [5], and tracking [6]. Successful metric learning needs to achieve the following two objectives: (1) *Discriminative*. In the embedded feature space, image features with the same

*Corresponding authors

semantic labels should be aggregated into compact clusters in the high-dimensional feature space while those from different classes should be well separated from each other. (2) *Generalizable*. The learned features should be able to generalize well from the training images to test images of new classes which have not been seen before. During the past a few years, methods based on deep neural networks, such as metric loss functions design [7, 8, 9, 10, 11], embedding transfer [12, 13, 14, 15, 16], structural matching [17], graph neural networks [2, 18], language guidance [19], and vision transformer [1, 20, 21], have achieved remarkable progress on learning discriminative features. However, the generalization onto unseen new classes remains a significant challenge for existing deep metric learning methods.

In the literature, to improve the deep metric learning performance and alleviate the generalization problem on unseen classes, regularization techniques [22, 15], language-guided DML [19], and feature fusion [2, 8, 18] methods have been developed. Existing approaches to addressing the generalization challenge in metric learning focus on the robustness of linear or kernel-based distance metrics [23, 24], analysis of error bounds of the generalization process [25], and correlation analysis between generalization and structure characteristics of the learned embedding space [22]. It should be noted that in existing methods, the input image is analyzed and transformed as a whole into an embedded feature. In other words, the image is represented and projected globally from a single perspective. We recognize that this single-perspective projection is not able to represent and encode the highly complex and dynamic correlation structures in the high-dimensional feature space since they are being collapsed and globally projected onto one single perspective and the local correlation dynamics have been suppressed. According to our experiments, this single-perspective global projection will increase the marginal variance [26] and consequently degrade the generalization capability of the deep metric learning method.

Furthermore, we observe that existing deep metric learning methods attempt to transform and encode the original features. From the generalization point of view, we find that it is more effective to learn the embedding based on relative difference between features since the absolute value of features may vary significantly from the training to new test classes, but the relative change patterns between features may remain largely invariant. To further understand this idea, consider the following toy example: a face in the daytime may appear much different from a face in the night time due to changes in lighting conditions. However, an effective face detection with sufficient generalization power will not focus on the absolute pixel values of the face image. Instead, it detects the face based on the relative change patterns between neighboring regions inside the face image. Motivated by this observation, in this work, to address the generalization challenge, we propose to learn the embedded feature from the projection residuals of the feature map, instead of its absolute features.

The above two ideas, namely, multi-perspective projection and residual encoding, lead to our proposed method of coded residual transform for deep metric learning. Specifically, we propose to learn a set of diversified prototype features, project the features onto every prototype, and then encode the features using the projection residuals weighted by their correlation coefficients with the target prototype. Unlike existing transformer-based feature representation approaches which encode the original values of features based on global correlation analysis [27, 28, 29], the proposed coded residual transform encodes the relative differences between original features and their projected prototypes. Our extensive experimental results and ablation studies demonstrate that the proposed CRT method is able to improve the generalization performance of deep metric learning, outperforming the state-of-the-art methods by large margins and improving upon the current best method by up to 4.28%.

We learn those projection prototypes based on the training classes and transfer them into the test classes. Although the training and test classes share the same set of prototypes, the actual distributions of project prototypes during training and testing could be much different due to the distribution shift between the training and testing classes. During our coded residual transform, we assign different weights for different project residuals based on the correlation between the feature and the corresponding prototype. Therefore, for training classes, the subset of prototypes which are close to the training images will have larger weights. Similarly, for the testing classes, the subset of prototypes which are close to the test images will have larger weights. This correlation-based weighting for the projection residual contribute significantly to the overall performance gain.

2 Related Work and Unique Contributions

This work is related to deep metric learning, transformer-based learning methods, and residual encoding. In this section, we review the existing methods on these topics and discuss the unique novelty of our approach.

(1) Deep metric learning. Deep metric learning aims to learn discriminative features with the goal to minimize intra-class sample distance and maximize inter-class sample distance in a contrastive manner. Contrastive loss [30] has been successfully used in early methods of deep metric learning, aiming to optimize pairwise distance of between samples. By exploring more sophisticated relationship between samples, a variety of metric loss functions, such as triplet loss [31], lifted structured loss [32], proxy-anchor loss [9], and multi-similarity (MS) loss [11], have been developed. According to the studies in [22] and [33], the MS loss was verified to be one of the most efficient metric loss functions. Some recent methods explore how to use multiple features to learn robust feature embeddings. Kan *et al.* [2] and Seidenschwarz *et al.* [18] adopt K-nearest neighbors (k-NN) of an anchor image to build local graph neural network (GNN) and refine embedding vectors based on message exchanges between the graph nodes. Zhao *et al.* [17] proposed a structural matching method to learn a metric function between feature maps based on the optimal transport theory. Based on the form of softmax, margin-based softmax loss functions [34, 35, 36] were also proposed to learn discriminative features. Sohn [37] improved the contrastive loss and triplet loss by introducing N negative examples and proposed the N-pair loss function to speed up model convergence during training.

(2) Transformer-based learning methods. This work is related to transformer-based learning methods since our method also analyze the correlation between features and uses this correlation information to aggregate features. The original work of transformer [27] aims to learn a self-attention function and a feed forward transformation network for nature language processing. Recently, it has been successfully applied to computer vision and image processing. ViT [38] demonstrates that a pure transformer can achieve state-of-the-art performance in image classification. ViT treats each image as a sequence of tokens and then feeds them to multiple transformer layers to perform the classification. Subsequently, DeiT [39] further explores a data-efficient training strategy and a distillation approach for ViT. More recent methods such as T2T ViT [29], TNT [40], CrossViT [41] and LocalViT [42] further improve the ViT method for image classification. PVT [43] incorporates a pyramid structure into the transformer for dense prediction tasks. After that, methods such as Swin [28], CvT [44], CoaT [45], LeViT [46], Twins [47] and MiT [48] enhance the local continuity of features and remove fixed size position embedding to improve the performance of transformers for dense prediction tasks. For deep metric learning, El-Nouby *et al.* [1] and Ermolov *et al.* [20] adopt the DeiT-S network[39] as a backbone to extract features, achieving impressive performance.

(3) Residual encoding. Residual encoding was first proposed by Jégou *et al.* [49], where the vector of locally aggregated descriptors (VLAD) algorithm is used to aggregate the residuals between features and their best-matching codewords. Based on the VLAD method, VLAD-CNN [50] has developed the residual encoders for visual recognition and understanding tasks. NetVLAD [51] and Deep-TEN [52] extend this idea and develop an end-to-end learnable residual encoder based on soft-assignment. It should be noted that features learned by these methods typically have very large sizes, for example, 16k, 32k and 4096 for AlexNet [53], VGG-16 [54] and ResNet-50 [55], respectively.

(4) Unique Contributions. Compared to the above existing methods, the unique contributions of this paper can be summarized as follows: (1) We introduce a new CRT method which learns a set of prototype features, project the feature map onto each prototype, and then encode its features using their projection residuals weighted by their correlation coefficients with each prototype. (2) We introduce a diversity constraint for the set of prototype features so that the CRT method can represent and encode the feature map from a set of complimentary perspectives. Unlike existing transformer-based feature representation approaches which encode the original values of features based on global correlation analysis, the proposed coded residual transform encode the relative differences between original features and their projected prototypes. (3) To further enhance the generalization performance, we propose to enforce the feature distribution consistency between coded residual transforms with different sizes of projection prototypes and embedding dimensions. (4) We demonstrate that this multi-perspective projection with diversified prototypes and coded residual representation based on relative differences are able to achieve significantly improved generalization

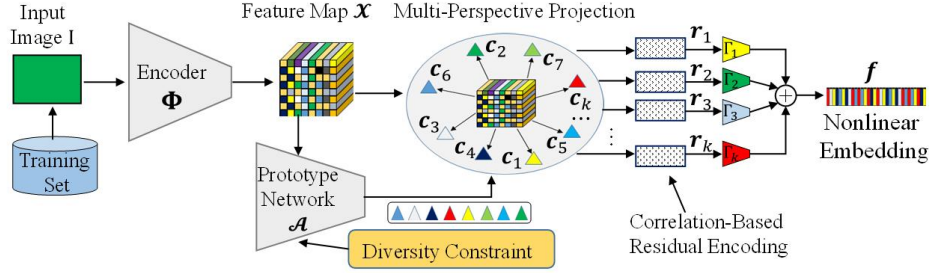


Figure 1: Overview of the proposed Coded residual transform (CRT) for generalizable deep metric learning.

capability in metric learning. Our proposed CRT method outperforms the state-of-the-art methods by large margins and improving upon the baseline method by up to 4.28%.

3 Method

In the following sections, we present our proposed method of coded residual transform for deep metric learning.

3.1 Method Overview

Figure 1 provides an overview of the proposed CRT method. We first use a backbone network Φ to encode the input image and extract its feature map $\mathcal{X} \in \mathbb{R}^{H \times W \times L}$, which consists of $H \times W$ feature vectors of size L . To improve the generalization capability of deep metric learning on feature map, we learn a prototype network to generate a set of diversified prototype features $\{c_1, c_2, \dots, c_K\}$ from the training set. Here, by "diversified" we mean these prototypes are able to provide multi-perspective complimentary representation of image features. We then project all feature vectors in the feature map onto each prototype c_k and encode them using the projection residuals weighted by their correlation coefficients with respect to this prototype. Each prototype c_k will generate a coded residual representation r_k of the feature map. After being further processed by a nonlinear embedding network Γ_k , these coded residual representations will be added together to form the final nonlinear feature embedding. The above feature embedding process is referred to as *coded residual transform*. To further enhance the generalization performance, we introduce a consistency constraint between two different coded residual transform with different values of K which is the size of the prototype set. In the following sections, we will explain the above major components of our CRT method in more details.

3.2 Multi-Perspective Projection and Correlation-Based Residual Encoding

Given an input image I , a backbone network Φ is used to encode image I into a feature map $\mathcal{X} \in \mathbb{R}^{H \times W \times L}$, i.e., $\mathcal{X} = \Phi(I)$. First, we learn prototype network to generate a set of diversified prototype features $\mathcal{C} = \{c_1, c_2, \dots, c_K\}$, $c_k \in \mathbb{R}^L$, whose learning process will be explained in the following section. For each prototype c_k , we project the whole feature map \mathcal{X} onto this prototype. Specifically, for each feature $x_j \in \mathcal{X}$ inside the feature map, we find the relative difference $d_{kj} = x_j - c_k$ between the feature x_j and the prototype c_k . Let $w_{kj} = x_j \cdot c_k^T$ be their correlation coefficient. Then, with prototype c_k , the whole map is transformed into the following feature vector using weighted summation of d_{kj} :

$$r_k = \sum_{j=1}^{H \times W} \log[1 + \exp(w_{kj})](x_j - c_k), \quad (1)$$

where the nonlinear function $\log[1 + \exp(w_{kj})]$ converts the correlation coefficient w_{kj} into a positive number. In this way, each prototype c_k will generate a separate coded residual representation r_k of the feature map for the input image. Finally, r_k is further transformed by a nonlinear embedding

network Γ_k with multiple fully connected layers and one GELU nonlinear activation layer [56]. By aggregating those nonlinear embeddings, the final embedded feature f is then given by

$$f = \frac{1}{K} \sum_{k=1}^K \Gamma_k(\mathbf{r}_k). \quad (2)$$

The task of the prototype network is to generate an optimized set of prototypes. Its input is the features from the feature map. Its weights are the prototypes that need to be learned, and its output is the correlations between the input features and the weights, which are the correlations between the feature map and prototype. The prototype network will update these prototypes using stochastic gradient descent (SGD) algorithm in back propagation. In this work, we use an one-layer fully connected network to implement this prototype network. The regularization of prototypes will be discussed in the following section.

Figure 2 shows two sets of examples of correlation map between different prototypes and the feature map. Each image corresponds to one prototype. The heat map shows the correlation between the prototype and the feature at the corresponding spatial location from the feature map. We can see that different prototypes are capturing different semantic components of the image and the feature map is projected and encoded from a large set of different semantic perspectives. Our generalization analysis and ablation studies will demonstrate that this multi-perspective projection and encoding will provide significantly enhanced generalization capability and improved metric learning performance.



Figure 2: Correlation heat maps between a learned set of prototypes (corresponding to 8 prototypes) and feature maps of two images. We can see that different prototypes response to different local or global views. The red dots on the top right corner indicates the background prototype.

3.3 Network Model Learning and Generalization Analysis

As illustrated in Figure 1, our proposed CRT method involves the encoder network Φ , the prototype network \mathcal{A} , and the multi-perspective feature embedding networks $\{\Gamma_k\}$. These networks are jointly trained in an end-to-end manner. The task of the prototype network \mathcal{A} is to generate a set of prototypes for efficient projection of the input features. From our experiments, we find that it is important to enforce diversity among these prototypes so that they can provide a diversified and robust representation of the image features. Diversity means that the prototype features have small correlation with each other. Let $\mathbf{C} = \{c_1, c_2, \dots, c_K\}$ be a set of prototypes generated by the prototype network. When training the prototype network, we need to minimize the following average correlation between these prototype features, which is defined to be the prototype diversity loss

$$L_{DIV} = \frac{1}{K(K-1)} \sum_{k \neq j} \frac{|c_k \cdot c_j^T|}{\|c_k\|_2 \cdot \|c_j\|_2}, \quad (3)$$

where the cosine similarity is used to measure the correlation between two different prototype features. To train the overall feature embedding network, we use the multi-similarity (MS) loss [11], denoted by L_{MS} , as our metric loss function to minimize the similarity for negative pairs and maximize the similarity for positive pairs. Here, negative pairs are samples from different classes while positive pairs are samples from the same class. The prototype diversity loss L_{DIV} and the MS loss L_{MS} are combined to form the overall loss function $L = L_{DIV} + \lambda_1 L_{MS}$ for end-to-end training of our CRT network.

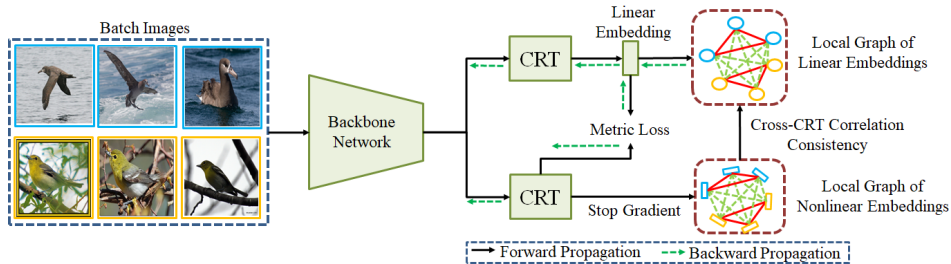


Figure 3: The training method of the proposed framework.

Table 1: The embedding space density (\uparrow) on the experimental datasets.

Method	CUB	Cars	SOP	In-Shop
Baseline	0.72	0.79	0.38	0.28
+CRT	0.90	1.01	0.40	0.33

Table 2: The spectral decay (\downarrow) on the experimental datasets.

Method	CUB	Cars	SOP	In-Shop
Baseline	0.27	0.24	0.31	0.23
+CRT	0.19	0.15	0.13	0.10

Cross CRT consistency loss. To further enhance the generalization performance, we propose to enforce the feature distribution consistency between coded residual transforms with different sizes of projection prototypes. As shown in Figure 3, we construct two CRT embedding branches with different number of projection prototypes. For example, in our experiment, the first branch has a prototype set size $K_1 = 49$ with an embedded feature size of 128, while the second branch has a prototype set size $K_2 = 64$ with an embedded feature size of 1024. Suppose that the current training batch of images are $\mathcal{I} = \{I_1, I_2, \dots, I_N\}$. Let the feature embeddings of the first CRT branch be $\{\mathbf{f}_1^{(1)}, \mathbf{f}_2^{(1)}, \dots, \mathbf{f}_N^{(1)}\}$ and the feature embeddings of the second branch be $\{\mathbf{f}_1^{(2)}, \mathbf{f}_2^{(2)}, \dots, \mathbf{f}_N^{(2)}\}$.

Define the similarity matrix

$$\mathbb{S}^{(1)} = \left[\mathbf{s}_{ij}^{(1)} \right]_{1 \leq i, j \leq N}, \quad \mathbf{s}_{ij}^{(1)} = \frac{\mathbf{f}_i^{(1)} \cdot [\mathbf{f}_j^{(1)}]^T}{\|\mathbf{f}_i^{(1)}\|_2 \cdot \|\mathbf{f}_j^{(1)}\|_2}. \quad (4)$$

Similarly, we can define the similarity matrix for the second branch as $\mathbb{S}^{(2)}$. The consistency between these two CRT branches are defined to be the L_1 distance between these two similarity matrices

$$L_{CON} = \|\mathbb{S}^{(1)} - \mathbb{S}^{(2)}\|_1. \quad (5)$$

This consistency loss is then combined with the original loss function for the CRT network. Thus, the overall loss is given by $L = L_{DIV} + \lambda_1 L_{MS} + \lambda_2 \cdot L_{CON}$.

Generalization capability analysis. In this section, we analyze the generalization capability of our proposed CRT method. Roth *et al.* [22] established two metrics to measure the generalization capability of deep metric learning methods: (1) embedding space density and (2) spectral decay. Methods with higher embedding space density and smaller spectral decay often have better generalization capabilities. The embedding space density metric \mathcal{D}_{ESD} is defined as the ratio between the average of intra-class distance \mathcal{D}_{Intra} and the average of inter-class distance \mathcal{D}_{Inter} :

$$\mathcal{D}_{ESD} = \mathcal{D}_{Intra} / \mathcal{D}_{Inter}. \quad (6)$$

The spectral decay metric ρ_{SD} is defined to be the KL-divergence between the spectrum of d singular values V^{SV} (obtained from Singular Value Decomposition, SVD) and a d -dimensional uniform distribution μ_d . It is inversely related to the entropy of the embedding space:

$$\rho_{SD} = \mathcal{D}_{KL}(\mu_d, V^{SV}). \quad (7)$$

Table 1 and Table 2 show the embedding space density and the spectral decay values of the feature embedding learned by the baseline method and our CRT method on the test datasets used in our experiments. We can see that our method achieves significantly higher embedding space density and much lower spectral decay when the model tested on unseen classes, which indicates significantly improved generalization capability.

4 Experimental Results

Following the same procedure of existing papers [2, 7, 13, 18, 20], we evaluate the performance of our proposed CRT method on four benchmark datasets for image retrieval tasks.

4.1 Datasets and Experimental Settings

(1) Datasets. In the following experiments, we use the same benchmark datasets as in existing papers for direct performance comparison. Four datasets, i.e., CUB-200-2011 [57], Cars-196 [58], Stanford Online Products (SOP) [32], and In-Shop Clothes Retrieval (In-Shop) [59], are used to our experiments. We use the same training and test split as in existing papers. Hyperparameters were determined previous to the result runs using a 80-20 training and validation split.

(2) Performance metrics and experimental settings. Following the standard protocol in [2, 7, 13, 18, 20, 60], the Recall@K [61] is used to evaluate the performance of our algorithm. For all datasets, our method is evaluated with the image data only, without using the bounding box information. During training, we randomly sample a set of images in each iteration to train the network. In each iteration, we first randomly choose the image classes, and then randomly sample 5 images from each class to form a batch. For the CUB and Cars datasets, we sampled 16 classes in a batch. For the SOP and In-Shop datasets, we sampled 36 classes in a batch. We apply random cropping with random flipping and resizing to 227×227 for all training images. For testing, we only use the center-cropped image to compute the feature embedding. Unless otherwise specified, we use the MixTransformer-B2 (MiT-B2) developed in [48] as our baseline encoder network with its pyramid MLP head being removed. Our CRT algorithm operates on the feature map generated by the last block (the 4-th block) of the backbone encoder network. The initial learning rate is $3e^{-5}$. For all images, the MS loss weight λ_1 in the first embedding branch is set as 1.0. In second embedding branch, it is set as 0.1 for the CUB and Cars datasets, and 0.9 for the SOP and In-Shop datasets. The consistency loss weight λ_2 is set to 0.9. The backbone network is pre-trained on the ImageNet-1K dataset.

4.2 Performance Comparisons with the State-of-the-art Methods

We compare the performance of our CRT method with the state-of-the-art deep metric learning methods. Performance comparison results on the CUB and Cars datasets are shown in Table 3. Table 4 shows the comparison results on the SOP and In-Shop datasets. It should be noted that the feature dimension of our CRT method is set to be 128. We can see that our CRT method significantly outperforms the current best deep metric learning method Hyp-DeiT [20]. The results of the Hyp-DeiT method are cited under the same experimental settings where the embedding size is 128 with image size of 227×227 , and a pretrained model on the ImageNet-1K. We choose this setting so that we can compare our method with many recent papers on metric learning. For example, on the CUB dataset, the top-1 recall rate has been improved by 4.28%. The experimental results on the rest datasets suggest that our CRT method consistently outperforms other deep metric learning methods by large margins.

As analyzed in [22] and [33], most of the deep metric learning methods use different experimental conditions, such as different settings of batch size, data augmentation methods, embedding sizes, training strategies, backbone networks, and input image sizes, to obtain the state-of-the-art performance, which could lead to confusion on the effectiveness of those methods. For example, Hyp-DeiT [20] and IRT_R [1] used larger batch sizes and memory bank technique to obtain better performance. The method of XBM+RTT [21] used the re-rank technique to obtain the highest top-1 recall rate on the SOP dataset. The Group Loss++ [7] also used the re-rank method to improve the retrieval performance. Moreover, Proxy-Anchor [9], Group Loss++ [7] and ETLR [13] used mixed pooling methods to improve embedding performance. During our experiments, we find that it is challenging to re-produce their original results with our available computing resources and to conduct fair comparisons, especially for those methods without publicly available source code. Instead, we implement our CRT method with the MS method [11] which has been extensively used in existing deep metric learning methods. In the following, we provide a fair comparison between our method and the baseline MS method with different backbone networks under the same experimental conditions.

Table 3: Comparison of retrieval performance on the CUB and Cars datasets.

Methods	Dim	CUB				Cars			
		R@1	R@2	R@4	R@8	R@1	R@2	R@4	R@8
A-BIER [TPAMI20] [60]	512	57.5	68.7	78.3	82.6	82.0	89.0	93.2	96.1
MS [CVPR19] [11]	512	65.7	77.0	86.3	91.2	84.1	90.4	94.0	96.5
Proxy-Anchor [CVPR20] [9]	512	68.4	79.2	86.8	91.6	86.1	91.7	95.0	97.3
DRML-PA [ICCV21] [62]	512	68.7	78.6	86.3	91.6	86.9	92.1	95.2	97.4
ETLR [CVPR21] [13]	512	72.1	81.3	87.6	-	89.6	94.0	96.5	-
DCML-MDW [CVPR21] [63]	512	68.4	77.9	86.1	91.7	85.2	91.8	96.0	98.0
D & C [TPAMI21] [64]	512	68.4	78.7	86.0	91.6	87.8	92.5	95.4	-
IBC [ICML21] [18]	512	70.3	80.3	87.6	92.7	88.1	93.3	96.2	98.2
LSCM-GNN [TIP22] [2]	512	68.5	77.3	85.3	91.3	87.4	91.5	94.9	97.0
Group Loss++ [TPAMI22] [7]	512	72.6	80.5	86.2	91.2	90.4	93.8	96.0	97.5
IRT _R [arXiv21] [1]	384	74.7	82.9	89.3	93.3	-	-	-	-
PA+DIML [ICCV21] [17]	128	66.46	-	-	-	86.13	-	-	-
Hyp-DeiT[CVPR22] [20]	128	74.7	84.5	90.1	94.1	82.1	89.1	93.4	96.3
Ours: CRT	128	78.98	86.68	91.61	95.04	91.16	94.92	96.79	98.03
Ours: Gain	128	4.28	2.18	1.51	0.94	0.76	0.92	0.29	-0.17

Table 4: Comparison of retrieval performance on the SOP and In-Shop datasets.

Methods	Dim	SOP				In-Shop			
		R@1	R@10	R@100	R@1000	R@1	R@10	R@20	R@30
Fusing-Net [TIP19] [8]	512	71.8	86.3	94.1	98.2	82.4	95.1	96.7	97.4
A-BIER [TPAMI20] [60]	512	74.2	86.9	94.0	97.8	83.1	95.1	96.9	97.5
MS [CVPR19] [11]	512	78.2	90.5	96.0	98.7	89.7	97.9	98.5	98.8
DRML-PA [ICCV21] [62]	512	71.5	85.2	93.0	-	-	-	-	-
ETLR [CVPR21] [13]	512	79.8	91.1	96.3	-	-	-	-	-
DCML-MDW [CVPR21] [63]	512	79.8	90.8	95.8	-	-	-	-	-
D & C [TPAMI21] [64]	512	79.8	90.4	95.2	-	90.4	97.6	-	-
IBC [ICML21] [18]	512	81.4	91.3	95.9	-	92.8	98.5	99.1	99.2
LSCM-GNN [TIP22] [2]	512	79.7	90.5	95.7	98.4	92.4	98.5	99.1	99.3
Group Loss++ [TPAMI22] [7]	512	79.2	90.1	95.8	-	90.9	97.6	98.4	98.9
IRT _R [arXiv21] [1]	384	84.0	93.6	97.2	99.1	91.5	98.1	98.7	99.0
PA+DIML [ICCV21] [17]	128	79.22	-	-	-	-	-	-	-
XBM+RTT [ICCV21] [21]	128	84.5	93.2	96.6	99.0	-	-	-	-
Hyp-DeiT[CVPR22] [20]	128	83.0	93.4	97.5	99.2	90.9	97.9	98.6	98.9
Ours: CRT	128	83.41	93.86	97.66	99.31	94.48	99.37	99.68	99.75
Ours: Gain	128	-1.09	0.26	0.16	0.11	1.68	0.87	0.58	0.45

4.3 Performance Comparisons with Different Backbone Networks.

We conduct experiments with different backbone networks to verify the effectiveness of the proposed CRT method. For fair comparisons [22, 33], we reproduce the MS method [11] and compare the performance using the same experimental settings. The hyper-parameter settings are consistent with the original paper [11]. The batch size is set to 80 on the CUB and Cars datasets, and 180 on the SOP and In-Shop datasets. The embedded feature size is set to 128. Results are shown in Table 5, we can see that our proposed method is able to consistently improve the performance of the baseline method. It should be noted that the DeiT-S and MiT-B1 networks are both based on the transformer, a powerful method for exploiting the global correlation between features for very efficient image representation. From Table 5, we can see that, even on top of these two baseline methods with the powerful transformer backbone network, our coded residual transform is still able to improve the metric learning performance by up to 3.7%, which is quite impressive. This is because our CRT method introduces the new ideas of multi-perspective projection and residual encoding, which have significantly improved the generalization performance of the deep metric learning.

4.4 Ablation Studies

In this section, we provide extensive ablation studies to further understand our proposed CRT method and characterize the performance of major algorithm components. In the following experiments, unless otherwise specified, the batch size N is set to 80. The backbone network used in this experiment is the MiT-B1.

Table 5: Comparisons of Recall@K (%) on the CUB, Cars, SOP and In-Shop datasets for different backbone networks.

Backbones	Methods	CUB			Cars			SOP			In-Shop		
		R@1	R@2	R@4	R@1	R@2	R@4	R@1	R@10	R@100	R@1	R@10	R@20
GoogLeNet	MS	56.53	69.13	79.54	76.49	84.76	90.38	70.10	85.73	94.41	87.33	97.73	98.56
	+CRT	59.23	71.02	81.52	78.50	86.35	91.91	71.06	86.41	94.73	88.31	97.83	98.68
	Gain	2.7	1.89	1.98	2.01	1.59	1.53	0.96	0.68	0.32	0.98	0.1	0.12
BN-Inception	MS	61.95	72.59	82.44	80.59	87.50	92.63	74.10	88.46	95.43	90.75	98.52	99.06
	+CRT	65.78	76.72	85.31	81.38	88.38	93.08	75.65	89.04	95.64	91.52	98.61	99.19
	Gain	3.83	4.13	2.87	0.79	0.88	0.45	1.55	0.58	0.21	0.77	0.09	0.13
ResNet-50	MS	62.64	73.73	83.20	79.92	87.63	92.41	76.49	89.33	95.66	90.11	97.52	98.27
	+CRT	64.20	75.54	84.12	83.29	89.76	93.88	78.97	91.10	96.51	92.38	98.77	99.25
	Gain	1.56	1.89	0.92	3.37	2.13	1.47	2.48	1.77	0.85	2.27	1.25	0.98
DeiT-S	MS	72.32	82.43	89.20	82.20	89.34	93.76	79.56	91.63	96.87	92.47	98.72	99.21
	+CRT	74.71	83.83	89.65	84.26	90.95	94.90	81.60	92.65	97.20	93.31	98.98	99.35
	Gain	2.39	1.4	0.45	2.06	1.61	1.14	2.04	1.02	0.33	0.84	0.26	0.14
MiT-B1	MS	72.25	81.85	88.54	87.36	92.26	95.23	79.67	91.55	96.66	92.20	98.64	99.21
	+CRT	75.95	84.47	90.26	89.60	94.20	96.47	82.32	93.02	97.19	93.51	99.11	99.50
	Gain	3.7	2.62	1.72	2.24	1.94	1.24	2.65	1.47	0.53	1.31	0.47	0.29

Table 6: The Recall@K (%) for different component on the CUB dataset.

Model	CUB			
	R@1	R@2	R@4	R@8
The Proposed Method	75.95	84.47	90.26	94.51
-CRT	73.97	84.03	90.41	94.31
-CRT-Consistency	72.25	81.85	88.54	93.57

Table 7: The Recall@K (%) with (w) and without (w/o) using multi-perspective CRT feature transformation.

	CUB			
	R@1	R@2	R@4	R@8
w/o	74.34	83.59	90.23	94.14
w	75.95	84.47	90.26	94.51

(1) Contributions of major algorithm components. From the performance evaluation perspective, our algorithm has two major components, the coded residual transform (CRT) and cross-CRT correlation consistency (CRT-Consistency). We fix the MS loss weight λ_1 in the first and second embedding branches as 1.0 and 0.1, respectively. The consistency loss weight λ_2 is set to be 0.9. From Table 6, we can see that the performance dropped 1.98% for the top-1 recall rate without the CRT. The performance future dropped 1.69% for the top-1 recall rate without the CRT-Consistency, which is the baseline result that obtained based on the MS loss function. Moreover, the multi-perspective CRT features transformation plays an important role for the final performance. For different projection prototypes, the CRT features can be transformed using different embedding networks or the same embedding network. Here, we compare the performance of our CRT method with and without using the same embedding network for the transformation of CRT features. Results are shown in Table 7. We can see that better performance can be obtained using different embedding networks for each CRT feature corresponding to each projection prototype. This shows the effectiveness of our multi-perspective projection.

(2) Impact of the projection prototypes. In this experiment, we analyze the impact of different numbers of projection prototypes. Table 8 and Table 9 show the results of different numbers of projection prototypes for the first embedding branch (low-dimensional embedding branch) and the second embedding branch (high-dimensional embedding branch), respectively. In Table 8, the number of projection prototypes in the second embedding branch is fixed at 64. This table reports the results of embedding computed from the first embedding branch when the number of projection prototypes changed from 1 to 64. The weights of the backbone networks are shared and the weights of the CRT heads are not shared for this experiment. In Table 9, the number of project prototypes are equal for the first and the second CRT embedding branches, which are changed from 1 to 100, and the weights of both the backbone network and the CRT branches are shared in this experiment. We can see that when the number of prototypes is set to be 64, the embedding performance reaches to the best.

In Table 9, the network weight of the second embedding branch is shared from the first embedding branch. Here, we compare the performance of our CRT method with and without shared weights between these two embedding branches. Results are shown in Table 10. We can see that the performance remains almost the same between these two study cases. In other experiments, to decrease the memory consumption, we shared weights for all the experiments.

Table 8: The Recall@K (%) for different number of projection prototypes in the first embedding branch.

K_1	CUB			
	R@1	R@2	R@4	R@8
1	75.76	84.52	90.72	94.78
4	75.57	84.30	90.56	94.33
16	75.44	84.25	90.24	94.46
64	75.96	84.60	90.75	94.31

Table 9: The Recall@K (%) for different number of projection prototypes in the second embedding branch.

K_2	CUB			
	R@1	R@2	R@4	R@8
1	74.26	84.30	89.82	93.96
4	74.54	84.03	90.06	94.01
16	74.63	83.74	90.24	94.02
64	75.95	84.47	90.26	94.51
100	75.15	84.35	90.36	94.31

Table 10: The Recall@K (%) with (w) and without (w/o) shared weights between these two embedding branches.

	CUB			
	R@1	R@2	R@4	R@8
w	75.95	84.47	90.26	94.51
w/o	75.96	84.60	90.75	94.31

5 Conclusion

In this paper, we have developed a coded residual transform for generalizable deep metric learning, which consists of a multi-perspective projection and coded residual transform encoder and a cross-CRT correlation consistency constraint. It has two unique characteristics. First, it represents and encodes the feature map from a set of complimentary perspectives based on projections onto diversified prototypes. Second, unlike existing transformer-based feature representation approaches which encode the original values of features based on global correlation analysis, the proposed coded residual transform encodes the relative differences between original features and their projected prototypes. The proposed CRT method has achieved new state-of-the-art metric learning performance on benchmark datasets. We hope our method can motivate further research. One limitation is that the memory and compute usage will be increased during training for these two embedding branches, and we shared weights between them to solve this problem in our experiments. Another limitation is that the projection prototypes were learned from the training set. It is unclear whether it is the best projection prototypes for new test classes. We leave it for the future work.

Acknowledgments

This work was supported in part by the National Key R&D Program of China 2021YFE0110500, in part by the National Natural Science Foundation of China under Grant 62202499, 61872034, 62062021 and 62011530042, in part by the Hunan Provincial Natural Science Foundation of China under Grant 2022JJ40632, in part by the Beijing Municipal Natural Science Foundation under Grant 4202055.

References

- [1] Alaaeldin El-Nouby, Natalia Neverova, Ivan Laptev, and Hervé Jégou. Training vision transformers for image retrieval. *arXiv*, abs/2102.05644, 2021.
- [2] Shichao Kan, Yigang Cen, YangLi, Mladenovic Vladimir, and Zhihai He. Local semantic correlation modeling over graph neural networks for deep feature embedding and image retrieval. *IEEE Trans. Image Processing*, 31:2988–3003, 2022.
- [3] Alec Radford, Jong Wook Kim, Chris Hallacy, Aditya Ramesh, Gabriel Goh, Sandhini Agarwal, Girish Sastry, Amanda Askell, Pamela Mishkin, Jack Clark, Gretchen Krueger, and Ilya Sutskever. Learning transferable visual models from natural language supervision. In *Proceedings of the 38th International Conference on Machine Learning, ICML 2021, 18-24 July 2021, Virtual Event*, volume 139, pages 8748–8763.
- [4] Shengcai Liao and Ling Shao. Graph sampling based deep metric learning for generalizable person re-identification. In *IEEE Conference on Computer Vision and Pattern Recognition, CVPR 2022, New Orleans, Louisiana, USA, June 21-24, 2022*, 2022.
- [5] Tianfei Zhou, Wenguan Wang, Ender Konukoglu, and Luc Van Gool. Rethinking semantic segmentation: A prototype view. In *IEEE Conference on Computer Vision and Pattern Recognition, CVPR 2022, New Orleans, Louisiana, USA, June 21-24, 2022*, 2022.
- [6] Yutao Cui, Cheng Jiang, Limin Wang, and Gangshan Wu. Mixformer: End-to-end tracking with iterative mixed attention. In *IEEE Conference on Computer Vision and Pattern Recognition, CVPR 2022, New Orleans, Louisiana, USA, June 21-24, 2022*, 2022.

- [7] Ismail Elezi, Jenny Seidenschwarz, Laurin Wagner, Sebastiano Vascon, Alessandro Torcinovich, Marcello Pelillo, and Laura Leal-Taixé. The group loss++: A deeper look into group loss for deep metric learning. *IEEE Trans. Pattern Anal. Mach. Intell.*, 2022.
- [8] Shichao Kan, Yigang Cen, Zhihai He, Zhi Zhang, Linna Zhang, and Yanhong Wang. Supervised deep feature embedding with handcrafted feature. *IEEE Trans. Image Processing*, 28(12):5809–5823, 2019.
- [9] Sungyeon Kim, Dongwon Kim, Minsu Cho, and Suha Kwak. Proxy anchor loss for deep metric learning. In *2020 IEEE/CVF Conference on Computer Vision and Pattern Recognition, CVPR 2020, Seattle, WA, USA, June 13-19, 2020*, pages 3235–3244, 2020.
- [10] Eu Wern Teh, Terrance DeVries, and Graham W. Taylor. Proxynca++: Revisiting and revitalizing proxy neighborhood component analysis. In *Computer Vision - ECCV 2020 - 16th European Conference, Glasgow, UK, August 23-28, 2020, Proceedings, Part XXIV*, volume 12369, pages 448–464, 2020.
- [11] Xun Wang, Xintong Han, Weilin Huang, Dengke Dong, and Matthew R. Scott. Multi-similarity loss with general pair weighting for deep metric learning. In *IEEE Conference on Computer Vision and Pattern Recognition, CVPR 2019, Long Beach, CA, USA, June 16-20, 2019*, pages 5022–5030, 2019.
- [12] Yuntao Chen, Naiyan Wang, and Zhaoxiang Zhang. Darkrank: Accelerating deep metric learning via cross sample similarities transfer. In *Proceedings of the Thirty-Second AAAI Conference on Artificial Intelligence, (AAAI-18), the 30th innovative Applications of Artificial Intelligence (IAAI-18), and the 8th AAAI Symposium on Educational Advances in Artificial Intelligence (EAAI-18), New Orleans, Louisiana, USA, February 2-7, 2018*, pages 2852–2859, 2018.
- [13] Sungyeon Kim, Dongwon Kim, Minsu Cho, and Suha Kwak. Embedding transfer with label relaxation for improved metric learning. In *IEEE Conference on Computer Vision and Pattern Recognition, CVPR 2021, virtual, June 19-25, 2021*, pages 3967–3976, 2021.
- [14] Wonpyo Park, Dongju Kim, Yan Lu, and Minsu Cho. Relational knowledge distillation. In *IEEE Conference on Computer Vision and Pattern Recognition, CVPR 2019, Long Beach, CA, USA, June 16-20, 2019*, pages 3967–3976, 2019.
- [15] Karsten Roth, Timo Milbich, Björn Ommer, Joseph Paul Cohen, and Marzyeh Ghassemi. Simultaneous similarity-based self-distillation for deep metric learning. In *Proceedings of the 38th International Conference on Machine Learning, ICML 2021, 18-24 July 2021, Virtual Event*, volume 139, pages 9095–9106, 2021.
- [16] Lu Yu, Vacit Oguz Yazici, Xialei Liu, Joost van de Weijer, Yongmei Cheng, and Arnau Ramisa. Learning metrics from teachers: Compact networks for image embedding. In *IEEE Conference on Computer Vision and Pattern Recognition, CVPR 2019, Long Beach, CA, USA, June 16-20, 2019*, pages 2907–2916, 2019.
- [17] Wenliang Zhao, Yongming Rao, Ziyi Wang, Jiwen Lu, and Jie Zhou. Towards interpretable deep metric learning with structural matching. In *2021 IEEE/CVF International Conference on Computer Vision, ICCV 2021, Montreal, QC, Canada, October 10-17, 2021*, pages 9867–9876, 2021.
- [18] Jenny Denise Seidenschwarz, Ismail Elezi, and Laura Leal-Taixé. Learning intra-batch connections for deep metric learning. In *Proceedings of the 38th International Conference on Machine Learning, ICML 2021, 18-24 July 2021, Virtual Event*, volume 139 of *Proceedings of Machine Learning Research*, pages 9410–9421, 2021.
- [19] Karsten Roth, Oriol Vinyals, and Zeynep Akata. Integrating language guidance into vision-based deep metric learning. In *IEEE Conference on Computer Vision and Pattern Recognition, CVPR 2022, New Orleans, Louisiana, USA, June 21-24, 2022*, 2022.
- [20] Aleksandr Ermolov, Leyla Mirvakhabova, Valentin Khulkov, Nicu Sebe, and Ivan V. Oseledets. Hyperbolic vision transformers: Combining improvements in metric learning. In *IEEE Conference on Computer Vision and Pattern Recognition, CVPR 2022, New Orleans, Louisiana, USA, June 21-24, 2022*, 2022.
- [21] Fuwen Tan, Jiangbo Yuan, and Vicente Ordonez. Instance-level image retrieval using reranking transformers. In *2021 IEEE/CVF International Conference on Computer Vision, ICCV 2021, Montreal, QC, Canada, October 10-17, 2021*, pages 12085–12095. IEEE, 2021.
- [22] Karsten Roth, Timo Milbich, Samarth Sinha, Prateek Gupta, Björn Ommer, and Joseph Paul Cohen. Revisiting training strategies and generalization performance in deep metric learning. In *Proceedings of the 37th International Conference on Machine Learning, ICML 2020, 13-18 July 2020, Virtual Event*, volume 119 of *Proceedings of Machine Learning Research*, pages 8242–8252, 2020.

- [23] Aurélien Bellet and Amaury Habrard. Robustness and generalization for metric learning. *Neurocomputing*, 151:259–267, 2015.
- [24] Shichao Kan, Linna Zhang, Zhihai He, Yigang Cen, Shiming Chen, and Jikun Zhou. Metric learning-based kernel transformer with triplets and label constraints for feature fusion. *Pattern Recognition*, 99, 2020.
- [25] Mengdi Huai, Hongfei Xue, Chenglin Miao, Liuyi Yao, Lu Su, Changyou Chen, and Aidong Zhang. Deep metric learning: The generalization analysis and an adaptive algorithm. In *Proceedings of the Twenty-Eighth International Joint Conference on Artificial Intelligence, IJCAI 2019, Macao, China, August 10-16, 2019*, pages 2535–2541, 2019.
- [26] Teng Zhang and Zhi-Hua Zhou. Optimal margin distribution machine. *IEEE Trans. Knowl. Data Eng.*, 32(6):1143–1156, 2020.
- [27] Ashish Vaswani, Noam Shazeer, Niki Parmar, Jakob Uszkoreit, Llion Jones, Aidan N. Gomez, Lukasz Kaiser, and Illia Polosukhin. Attention is all you need. In *Advances in Neural Information Processing Systems 30: Annual Conference on Neural Information Processing Systems 2017, December 4-9, 2017, Long Beach, CA, USA*, pages 5998–6008, 2017.
- [28] Ze Liu, Yutong Lin, Yue Cao, Han Hu, Yixuan Wei, Zheng Zhang, Stephen Lin, and Baining Guo. Swin transformer: Hierarchical vision transformer using shifted windows. In *2021 IEEE/CVF International Conference on Computer Vision, ICCV 2021, Montreal, QC, Canada, October 10-17, 2021*, pages 9992–10002, 2021.
- [29] Li Yuan, Yunpeng Chen, Tao Wang, Weihao Yu, Yujun Shi, Zihang Jiang, Francis E. H. Tay, Jiashi Feng, and Shuicheng Yan. Tokens-to-token vit: Training vision transformers from scratch on imagenet. In *2021 IEEE/CVF International Conference on Computer Vision, ICCV 2021, Montreal, QC, Canada, October 10-17, 2021*, pages 538–547, 2021.
- [30] Raia Hadsell, Sumit Chopra, and Yann LeCun. Dimensionality reduction by learning an invariant mapping. In *2006 IEEE Computer Society Conference on Computer Vision and Pattern Recognition (CVPR 2006), 17-22 June 2006, New York, NY, USA*, pages 1735–1742, 2006.
- [31] Florian Schroff, Dmitry Kalenichenko, and James Philbin. Facenet: A unified embedding for face recognition and clustering. In *IEEE Conference on Computer Vision and Pattern Recognition, CVPR 2015, Boston, MA, USA, June 7-12, 2015*, pages 815–823, 2015.
- [32] Hyun Oh Song, Yu Xiang, Stefanie Jegelka, and Silvio Savarese. Deep metric learning via lifted structured feature embedding. In *2016 IEEE Conference on Computer Vision and Pattern Recognition, CVPR 2016, Las Vegas, NV, USA, June 27-30, 2016*, pages 4004–4012, 2016.
- [33] Kevin Musgrave, Serge J. Belongie, and Ser-Nam Lim. A metric learning reality check. In Andrea Vedaldi, Horst Bischof, Thomas Brox, and Jan-Michael Frahm, editors, *Computer Vision - ECCV 2020 - 16th European Conference, Glasgow, UK, August 23-28, 2020, Proceedings, Part XXV*, volume 12370, pages 681–699, 2020.
- [34] Weiyang Liu, Yandong Wen, Zhiding Yu, and Meng Yang. Large-margin softmax loss for convolutional neural networks. In *Proceedings of the 33rd International Conference on Machine Learning, ICML 2016, New York City, NY, USA, June 19-24, 2016*, volume 48, pages 507–516, 2016.
- [35] Hao Wang, Yitong Wang, Zheng Zhou, Xing Ji, Dihong Gong, Jingchao Zhou, Zhifeng Li, and Wei Liu. Cosface: Large margin cosine loss for deep face recognition. In *2018 IEEE Conference on Computer Vision and Pattern Recognition, CVPR 2018, Salt Lake City, UT, USA, June 18-22, 2018*, pages 5265–5274, 2018.
- [36] Jiankang Deng, Jia Guo, Niannan Xue, and Stefanos Zafeiriou. Arcface: Additive angular margin loss for deep face recognition. In *IEEE Conference on Computer Vision and Pattern Recognition, CVPR 2019, Long Beach, CA, USA, June 16-20, 2019*, pages 4690–4699, 2019.
- [37] Kihyuk Sohn. Improved deep metric learning with multi-class n-pair loss objective. In *Advances in Neural Information Processing Systems 29: Annual Conference on Neural Information Processing Systems 2016, December 5-10, 2016, Barcelona, Spain*, pages 1849–1857, 2016.
- [38] Alexey Dosovitskiy, Lucas Beyer, Alexander Kolesnikov, Dirk Weissenborn, Xiaohua Zhai, Thomas Unterthiner, Mostafa Dehghani, Matthias Minderer, Georg Heigold, Sylvain Gelly, Jakob Uszkoreit, and Neil Houlsby. An image is worth 16x16 words: Transformers for image recognition at scale. In *9th International Conference on Learning Representations, ICLR 2021, Virtual Event, Austria, May 3-7, 2021*, 2021.

- [39] Nicolas Carion, Francisco Massa, Gabriel Synnaeve, Nicolas Usunier, Alexander Kirillov, and Sergey Zagoruyko. End-to-end object detection with transformers. In *Computer Vision - ECCV 2020 - 16th European Conference, Glasgow, UK, August 23-28, 2020, Proceedings, Part I*, volume 12346, pages 213–229, 2020.
- [40] Kai Han, An Xiao, Enhua Wu, Jianyuan Guo, Chunjing Xu, and Yunhe Wang. Transformer in transformer. In *Advances in Neural Information Processing Systems 34: Annual Conference on Neural Information Processing Systems 2021, NeurIPS 2021, December 6-14, 2021, virtual*, pages 15908–15919, 2021.
- [41] Chun-Fu (Richard) Chen, Quanfu Fan, and Rameswar Panda. Crossvit: Cross-attention multi-scale vision transformer for image classification. In *2021 IEEE/CVF International Conference on Computer Vision, ICCV 2021, Montreal, QC, Canada, October 10-17, 2021*, pages 347–356, 2021.
- [42] Yawei Li, Kai Zhang, Jiezhong Cao, Radu Timofte, and Luc Van Gool. Localvit: Bringing locality to vision transformers. *arXiv preprint, abs/2104.05707*, 2021.
- [43] Wenhai Wang, Enze Xie, Xiang Li, Deng-Ping Fan, Kaitao Song, Ding Liang, Tong Lu, Ping Luo, and Ling Shao. Pyramid vision transformer: A versatile backbone for dense prediction without convolutions. In *2021 IEEE/CVF International Conference on Computer Vision, ICCV 2021, Montreal, QC, Canada, October 10-17, 2021*, pages 548–558, 2021.
- [44] Haiping Wu, Bin Xiao, Noel Codella, Mengchen Liu, Xiyang Dai, Lu Yuan, and Lei Zhang. Cvt: Introducing convolutions to vision transformers. In *2021 IEEE/CVF International Conference on Computer Vision, ICCV 2021, Montreal, QC, Canada, October 10-17, 2021*, pages 22–31, 2021.
- [45] Weijian Xu, Yifan Xu, Tyler A. Chang, and Zhuowen Tu. Co-scale conv-attentional image transformers. In *2021 IEEE/CVF International Conference on Computer Vision, ICCV 2021, Montreal, QC, Canada, October 10-17, 2021*, pages 9961–9970, 2021.
- [46] Benjamin Graham, Alaaeldin El-Nouby, Hugo Touvron, Pierre Stock, Armand Joulin, Hervé Jégou, and Matthijs Douze. Levit: a vision transformer in convnet’s clothing for faster inference. In *2021 IEEE/CVF International Conference on Computer Vision, ICCV 2021, Montreal, QC, Canada, October 10-17, 2021*, pages 12239–12249, 2021.
- [47] Xiangxiang Chu, Zhi Tian, Yuqing Wang, Bo Zhang, Haibing Ren, Xiaolin Wei, Huaxia Xia, and Chunhua Shen. Twins: Revisiting the design of spatial attention in vision transformers. In *Advances in Neural Information Processing Systems 34: Annual Conference on Neural Information Processing Systems 2021, NeurIPS 2021, December 6-14, 2021, virtual*, pages 9355–9366, 2021.
- [48] Enze Xie, Wenhai Wang, Zhiding Yu, Anima Anandkumar, Jose M. Alvarez, and Ping Luo. Segformer: Simple and efficient design for semantic segmentation with transformers. *Advances in Neural Information Processing Systems 34*, 2021.
- [49] Hervé Jégou, Florent Perronnin, Matthijs Douze, Jorge Sánchez, Patrick Pérez, and Cordelia Schmid. Aggregating local image descriptors into compact codes. *IEEE Trans. Pattern Anal. Mach. Intell.*, 34(9):1704–1716, 2012.
- [50] Yunchao Gong, Liwei Wang, Ruiqi Guo, and Svetlana Lazebnik. Multi-scale orderless pooling of deep convolutional activation features. In *Computer Vision - ECCV 2014 - 13th European Conference, Zurich, Switzerland, September 6-12, 2014, Proceedings, Part VII*, volume 8695, pages 392–407, 2014.
- [51] Relja Arandjelovic, Petr Gronát, Akihiko Torii, Tomás Pajdla, and Josef Sivic. Netvlad: CNN architecture for weakly supervised place recognition. *IEEE Trans. Pattern Anal. Mach. Intell.*, 40(6):1437–1451, 2018.
- [52] Hang Zhang, Jia Xue, and Kristin J. Dana. Deep TEN: texture encoding network. In *2017 IEEE Conference on Computer Vision and Pattern Recognition, CVPR 2017, Honolulu, HI, USA, July 21-26, 2017*, pages 2896–2905. IEEE Computer Society, 2017.
- [53] Alex Krizhevsky, Ilya Sutskever, and Geoffrey E. Hinton. Imagenet classification with deep convolutional neural networks. *Commun. ACM*, 60(6):84–90, 2017.
- [54] Karen Simonyan and Andrew Zisserman. Very deep convolutional networks for large-scale image recognition. In *3rd International Conference on Learning Representations, ICLR 2015, San Diego, CA, USA, May 7-9, 2015, Conference Track Proceedings*, 2015.
- [55] Kaiming He, Xiangyu Zhang, Shaoqing Ren, and Jian Sun. Deep residual learning for image recognition. In *2016 IEEE Conference on Computer Vision and Pattern Recognition, CVPR 2016, Las Vegas, NV, USA, June 27-30, 2016*, pages 770–778. IEEE Computer Society, 2016.

- [56] Hendrycks Dan and Gimpel Kevin. Gaussian error linear units (gelus). *arXiv preprint*, abs/1606.08415, 2016.
- [57] Catherine Wah, Steve Branson, Peter Welinder, Pietro Perona, and Serge Belongie. The caltech-ucsd birds-200-2011 dataset. *California Institute of Technology*, pages 1–8, 2011.
- [58] Jonathan Krause, Michael Stark, Jia Deng, and Li Fei-Fei. 3d object representations for fine-grained categorization. In *2013 IEEE International Conference on Computer Vision Workshops, ICCV Workshops 2013, Sydney, Australia, December 1-8, 2013*, pages 554–561, 2013.
- [59] Ziwei Liu, Ping Luo, Shi Qiu, Xiaogang Wang, and Xiaoou Tang. Deepfashion: Powering robust clothes recognition and retrieval with rich annotations. In *2016 IEEE Conference on Computer Vision and Pattern Recognition, CVPR 2016, Las Vegas, NV, USA, June 27-30, 2016*, pages 1096–1104, 2016.
- [60] Michael Opitz, Georg Waltner, Horst Possegger, and Horst Bischof. Deep metric learning with BIER: boosting independent embeddings robustly. *IEEE Trans. Pattern Anal. Mach. Intell.*, 42(2):276–290, 2020.
- [61] Hervé Jégou, Matthijs Douze, and Cordelia Schmid. Product quantization for nearest neighbor search. *IEEE Trans. Pattern Anal. Mach. Intell.*, 33(1):117–128, 2011.
- [62] Zheng Wenzhao, Zhang Borui, Lu Jiwen, and Zhou Jie. Deep relational metric learning. In *Proceedings of the IEEE/CVF International Conference on Computer Vision (ICCV)*, pages 12065–12074, October 2021.
- [63] Wenzhao Zheng, Chengkun Wang, Jiwen Lu, and Jie Zhou. Deep compositional metric learning. In *IEEE Conference on Computer Vision and Pattern Recognition, CVPR 2021, virtual, June 19-25, 2021*, pages 9320–9329, 2021.
- [64] Artsiom Sanakoyeu, Pingchuan Ma, Vadim Tschernezki, and Björn Ommer. Improving deep metric learning by divide and conquer. *IEEE Trans. Pattern Anal. Mach. Intell.*, 2021.

Checklist

1. For all authors...
 - (a) Do the main claims made in the abstract and introduction accurately reflect the paper’s contributions and scope? [\[Yes\]](#) Abstract and Introduction
 - (b) Did you describe the limitations of your work? [\[Yes\]](#) Conclusion
 - (c) Did you discuss any potential negative societal impacts of your work? [\[Yes\]](#)
 - (d) Have you read the ethics review guidelines and ensured that your paper conforms to them? [\[Yes\]](#)
2. If you are including theoretical results...
 - (a) Did you state the full set of assumptions of all theoretical results? [\[N/A\]](#)
 - (b) Did you include complete proofs of all theoretical results? [\[N/A\]](#)
3. If you ran experiments...
 - (a) Did you include the code, data, and instructions needed to reproduce the main experimental results (either in the supplemental material or as a URL)? [\[Yes\]](#) Supplemental material
 - (b) Did you specify all the training details (e.g., data splits, hyperparameters, how they were chosen)? [\[Yes\]](#)
 - (c) Did you report error bars (e.g., with respect to the random seed after running experiments multiple times)? [\[Yes\]](#)
 - (d) Did you include the total amount of compute and the type of resources used (e.g., type of GPUs, internal cluster, or cloud provider)? [\[Yes\]](#)
4. If you are using existing assets (e.g., code, data, models) or curating/releasing new assets...
 - (a) If your work uses existing assets, did you cite the creators? [\[Yes\]](#)
 - (b) Did you mention the license of the assets? [\[Yes\]](#)
 - (c) Did you include any new assets either in the supplemental material or as a URL? [\[No\]](#)
 - (d) Did you discuss whether and how consent was obtained from people whose data you’re using/curating? [\[N/A\]](#)

- (e) Did you discuss whether the data you are using/curating contains personally identifiable information or offensive content? [N/A]
5. If you used crowdsourcing or conducted research with human subjects...
- (a) Did you include the full text of instructions given to participants and screenshots, if applicable? [N/A]
 - (b) Did you describe any potential participant risks, with links to Institutional Review Board (IRB) approvals, if applicable? [N/A]
 - (c) Did you include the estimated hourly wage paid to participants and the total amount spent on participant compensation? [N/A]